Atmos. Chem. Phys. Discuss., doi:10.5194/acp-2016-1085, 2017
Manuscript under review for journal Atmos. Chem. Phys.
Published: 5 January 2017

Atmospheric Chemistry and Physics Discussions

Experimental evidence of the rear capture of aerosol particles by raindrops

Pascal Lemaitre[1], Arnaud Querel[2*], Marie Monier[3,4], Thibaut Menard[5], Emmanuel Porcheron[1], Andrea I. Flossmann[3,4]

[1] Institut de Radioprotection et de Sûreté Nucléaire (IRSN), PSN-RES, SCA, LPMA, Gif-sur-Yvette, France
[2] Institut de Radioprotection et de Sûreté Nucléaire (IRSN), PRP-CRI, SESUC, BMCA, Fontenay-aux-Roses, France
[3] Clermont Université, Université Blaise Pascal, Laboratoire de Météorologie Physique, Clermont-Ferrand, France
[4] CNRS, INSU, UMR 6016, LaMP, Aubière, France
[5] CNRS UMR 6614 - CORIA Rouen, Site Universitaire du Madrillet, Saint Etienne du Rouvray, France
[*] Currently Strathom Energie, Paris, France
Correspondence to: P. Lemaitre (pascal.lemaitre@irsn.fr)

Abstract. This article presents new measurements of the efficiency with which aerosol particles of accumulation mode size are collected by a 1.25 mm sized raindrop. These laboratory measurements provide the link to reconcile the scavenging coefficients obtained from theoretical approaches with those from experimental studies. We provide here experimental proof of the rear capture mechanism in the flow around drops, which has a fundamental effect on sub-microscopic particles. These experiments thus confirm the efficiencies theoretically simulated by Beard (1974). Finally, we propose a semi-analytical expression to take into account this essential mechanism to calculate the collection efficiency for drops within the rain size range.

Introduction

Aerosol particles are an important component of the atmosphere. They significantly contribute to the Earth's energy budget, by directly interacting with solar radiation, as well as serving as precursors to cloud formation (Cloud condensation Nuclei, or CCN) which will in turn interact with this radiation (Twomey, 1974). Furthermore, the physical properties of these particles in suspension within the atmosphere (size, concentration, affinity for water, etc.) are essential parameters for characterizing air quality. These reasons have led the scientific community to actively study the physics of these atmospheric aerosol particles.

Aerosol particles originate in many ways. The primary natural sources are sea spray, wind-driven dust, volcanic eruptions and human activities. The secondary sources are associated with the gas-to-particle conversion of

Atmos. Chem. Phys. Discuss., doi:10.5194/acp-2016-1085, 2017
Manuscript under review for journal Atmos. Chem. Phys.
Published: 5 January 2017

Atmospheric Chemistry and Physics Discussions

certain gases present in the atmosphere. The size of these particles greatly varies and ranges from one nanometre to several hundred microns. Particles of anthropogenic origin represent an increasingly large proportion of aerosol particles in the atmosphere (Charlson *et al.* 1992, Wang *et al.* 2014). Of all man-made pollution, radioactive releases from a nuclear accident represent a particular hazard for humans and the environment. Just like all other particles, once emitted, radioactive particles undergo physical processes that drastically change their size distribution during their transport in the atmosphere. Ultrafine particles are very sensitive to Brownian diffusion and grow by coagulation. Large particles sediment on the ground under the effect of gravity. Hence, there is a particle size range that has a very long residence time in the atmosphere. This size range is referred to as the accumulation mode (Whitby, 1973). It is made up of particles with a diameter of between 0.1 µm and 2 µm. These particles can remain in the upper troposphere for several months (Jaenicke, 1988) and can be transported over long distances, crossing oceans and continents (Pruppacher *et al.*, 1998)

The accumulation of particles within this size range is essentially limited by two atmospheric processes: in-cloud scavenging (rainout) and below-cloud scavenging (washout) during rainfall events. Thus, in the event of a nuclear accident with radioactive aerosol release, it is essential to correctly model both of these mechanisms in order to predict their concentration within the troposphere (as well as ground contamination).

To start, we focus on the study of the below cloud scavenging of aerosol particles by rain. We adopt a micro-physical approach. We focus on the laboratory measurement of the collection efficiency of the aerosol particles constituting the accumulation mode, by drops of a size representative of rain. Recent measurements with 2 mm drops (Quérel *et al.* 2014b) have shown that for submicronic particles the collection efficiency increases very rapidly when the size of the particles reduces. The Slinn (1977) model does not reproduce this increase in efficiency, leading to errors of several orders of magnitude. We attribute this discrepancy to the key hypothesis of the model which assumes Stokes flow conditions around the drop. Yet, the Reynolds number of a 2 mm drop at its terminal velocity is approximately 800, this assumption of Stokes flow is therefore unjustified. This model nonetheless remains the most widely used in the literature mainly because it is easy to use.

Quérel *et al.* (2014b) showed that Beard (1974) model was the only one to predict this increase of the collection efficiency for submicronic aerosol particles. However, they were not able to perform collection efficiency measurements in the drop size range simulated by Beard (1974). Thus, they linearly extrapolated this model to compare with their measurements. This showed a satisfactory agreement, even for aerosol particles in the submicron range. The linear extrapolation is not completely satisfactory for an experimental validation of this model. Present article shows an experimental evidence of the robustness of K.V. Beard simulation for raindrop sizes originally investigated (diameter between 0.28 and 1.25 mm).

Our paper is divided into three sections. Firstly, we present a theoretical description of the problem of aerosol scavenging by rain. We then present out experimental set-up and the associated experimental results. Finally, we compare our measurements against the models in the literature in order, ultimately, to propose a semi-empirical correlation for calculating the elementary collection efficiency associated with rear capture.

Atmos. Chem. Phys. Discuss., doi:10.5194/acp-2016-1085, 2017
Manuscript under review for journal Atmos. Chem. Phys.
Published: 5 January 2017

Atmospheric Chemistry and Physics Discussions

1 Theoretical description of washout

At mesoscale, the scavenging of aerosol particles by rain is described by the scavenging coefficient (λ). This parameter is defined as the fraction of particles of diameter d_{ap} captured by the raindrops, per unit time (eq. 1). In this equation $C(d_{ap})$ is the concentration of aerosol particles of diameter d_{ap} in suspension in air per unit volume.

$$\frac{dC(d_{ap})}{C(d_{ap})} = -\lambda_{rain}(d_{ap})dt \qquad (1)$$

This parameter is essential for predicting the air quality (Chate, 2005) and the ground contamination following a nuclear accident with release of radionuclides into the environment (Groëll *et al.*, 2014; Quérel *et al.*, 2015). There are several approaches for determining this parameter. It can either be determined theoretically, by resolving equation (2) (Flossmann, 1986; Mircea *et al.*, 1998; 2000), or measured in the environment by monitoring the variation of particulate concentration in the atmosphere during precipitation (Volken & Schumann, 1993; Laakso *et al.*, 2003; Chate, 2005; Depuydt, 2013).

$$\lambda_{rain}(d_{ap}, D_{drop}) = \int_{D_{drop}=0}^{\infty} \frac{\pi {D_{drop}}^2}{4} \cdot U_{\infty}(D_{drop})\, E(d_{ap}, D_{drop}, RH) N(D_{drop}) dD_{drop} \qquad (2)$$

In this equation, D_{drop} is the drop diameter, $U_{\infty}(D_{drop})$ is the terminal fall velocity, $N(D_{drop})dD_{drop}$ is the concentration of drops with a diameter between D_{drop} and $D_{drop} + dD_{drop}$ during the rainfall event and $E(d_{ap}, D_{drop}, RH)$ is the efficiency of collection.

Unfortunately, these two approaches yield λ values, which differ by several orders of magnitude, in particular for submicron particles (Laakso *et al.*, 2003). It is clear, when we examine equations (1) and (2), that each of the two methods has advantages and significant limitations, which are also highlighted by the authors. The main limitation for measurement of the scavenging coefficient in the environment remains on the assumption that the change in concentration is related exclusively to collection by the drops. However, even if the rainfall events are methodically selected, it is difficult to completely neglect advection, turbulent transport, coagulation and the influence of particle hygroscopicity (Flossmann, 1991). For example, Quérel *et al.*, (2014a) have recently shown that during convective episodes, the downdraft was the main cause of the reduction in particulate concentration, well before collection by the drops.

In addition to the theoretical approach, the main limitation is the requirement to know the efficiency of collection (eq. 2). This microphysical parameter is defined as the ratio between the effective collection area (in other words, the cross-sectional area inside which the particle trajectory is intercepted by the drop) and the cross-sectional area of the drop. It is equivalent to defining the ratio of the mass of particles (of a given diameter) collected by the drop over the mass of particles (of the same diameter) within the volume swept by a sphere of equivalent volume (eq. 3).

$$E(d_{AP}, D_d, RH) = \frac{m_{AP,collected}(d_{AP})}{m_{AP,swept}(d_{AP})} \qquad (3)$$

Atmos. Chem. Phys. Discuss., doi:10.5194/acp-2016-1085, 2017
Manuscript under review for journal Atmos. Chem. Phys.
Published: 5 January 2017

Atmospheric Chemistry and Physics Discussions

However, there are many uncertainties associated with this parameter, in particular for raindrops. This is because, once they reach their terminal velocity, the Reynolds and the Webber numbers of these large drops are very high. Therefore, they oscillate at high frequency (Szakáll *et al.* 2010), which greatly complicates the simulation of flows inside and outside the drop. Furthermore, the boundary layer separation in the wake of the drop, results in significant recirculating flows. Therefore, there are currently few methods for numerically simulating such flows (although mention should be made of the work of Menard *et al.* 2007). The most common approach continues to be to use the Slinn model (Volken & Schumann, 1993; Laakso *et al.*, 2003; Chate, 2005; Depuydt, 2013), essentially for its ease of use and despite its strong assumptions. It should be kept in mind that Slinn models the flow around the drop as a Stokes flow, which translates in ignoring the convective terms of the Navier-Stokes equation. Such flows have a similar kinematic field to that of a potential flow. Slinn model cannot therefore capture the separation of the boundary layer in the wake of the drop. The flow on the front face of the drop is, however, relatively well modelled.

Moreover, Beard and Grover (1974) have developed a more sophisticated numerical model than Slinn (1977) to numerically simulate the collision between particles and a drop. The principle difference is that they do not assume Stokes flow. Flow around the drop is computed by resolving the complete Navier-Stokes equations (without ignoring the convective term). Beard and Grover (1974) do however make two simplifying assumptions: a spherical drop and axisymmetric flow. These simulations capture the separation of the boundary layer in the wake of the drop and the resulting recirculating flows. Using these simulations Beard (1974) derived the collision efficiencies between drops and particles of different sizes. For this, he calculated the trajectory of the particles in the flow by applying drag and gravity forces to them. The drag force is calculated from the Stokes-Cunningham expression to take into account the non-continuum effects, which are seen in the case of the smallest particles. These simulations highlight, for the first time, the capture of submicron-sized particles in the rear of the drop, due to wake recirculation.

The numerous measurements of efficiency found in the literature (Kerker and Hampl, 1974; Grover *et al.*, 1977; Wang and Pruppacher, 1977; Lai *et al.* 1978; Pranesha and Kamra, 1996; Vohl *et al.*, 1999) did not, until recently, allow to decide between these two models, as there are few measurements for submicron particles.

Recently, Quérel *et al.* (2014a) showed that the Slinn model underestimates by two orders of magnitude the measured collection efficiencies for submicron-sized particles. However, the Beard (1974) model, appears to be in agreement with their experimental results. Unfortunately, in order to make this comparison, Quérel *et al.* (2014a) were required to extrapolate the simulations of K.V. Beard.

In this paper, we investigate the collection efficiency for drops within the size range simulated by Beard (1974). The object of this paper is therefore to address these uncertainties in collection efficiency, by accurately measuring them in the laboratory, with the ultimate aim of theoretically deriving a scavenging coefficient.

2 Experimental set-up

The new experimental set-up follows the one described and deployed by Quérel (2014b). This facility is called BERGAME (French acronym for Facility to study the aerosol scavenging and to measure the collection efficiency).

Atmos. Chem. Phys. Discuss., doi:10.5194/acp-2016-1085, 2017
Manuscript under review for journal Atmos. Chem. Phys.
Published: 5 January 2017

Atmospheric Chemistry and Physics Discussions

The three stages are as follows and will be presented in the next subsections (Fig. 1):

- a mono-dispersed drop generator;
- a free-fall shaft;
- an aerosol chamber.

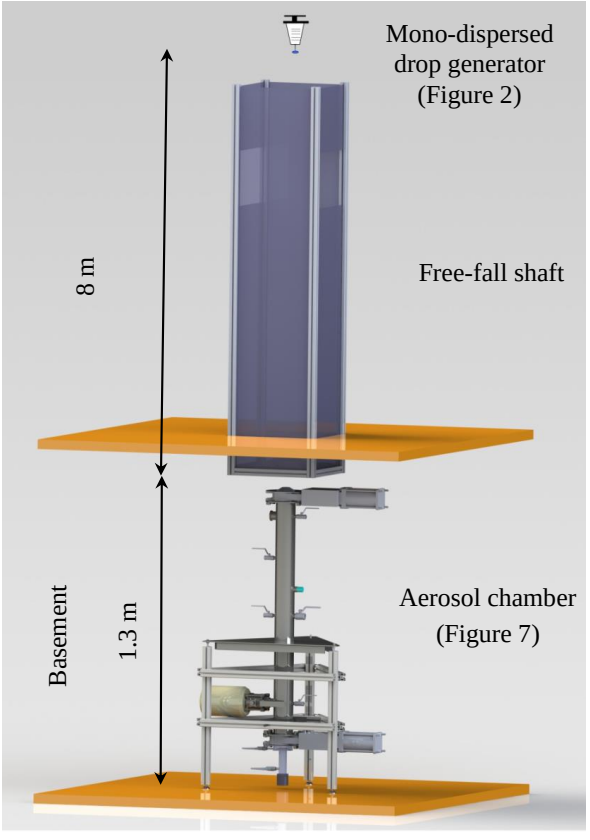

Figure 1: The new BERGAME set-up

The main changes with respect to Quérel *et al.* (2014b) concern the drop generator and the aerosol chamber. Indeed, those authors concluded that drops generation was one of the main points to improve, essentially to be able make direct comparisons with Beard (1974) simulations. As a consequence, the experimental setup has been improved to meet these requirements. Moreover an additional attention was drawn on the aerosol chamber. It has been modified not only to increase the particle number concentration, but also to better control the relative humidity, the aerosol neutralisation and finally to minimize the uncertainties. These two items of the BERGAME installation are described in the following sections.

Atmos. Chem. Phys. Discuss., doi:10.5194/acp-2016-1085, 2017
Manuscript under review for journal Atmos. Chem. Phys.
Published: 5 January 2017

Atmospheric Chemistry and Physics Discussions

2.1 Production of drops representative of rain

In order to enable the generation of finer drops, a new generator (Figure 2) was developed, characterised then installed at the top of the free-fall shaft of the BERGAME installation. This generator was placed 8 metres above the new aerosol chamber. The total height of the drop shaft has been reduced by 2 m because, as the drops are smaller than those investigated by Quérel *et al.* (2014a and b), they reach their terminal velocity in a shorter distance.

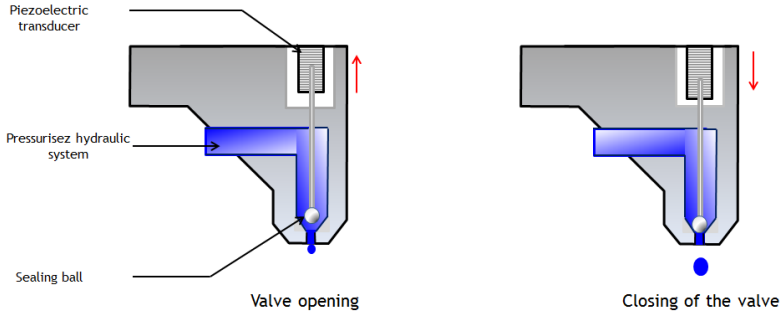

Figure 2. Diagram of operation of the generator opening valve

The generator consists of a valve operated by piezoelectric actuators which transmit its movement to a rod. A ceramic sealing ball is attached to the rod and opens together with the valve to enable the fluid to flow out of the valve (see Figure 2). The water circuit is maintained under pressure by the compressed air system.

In order to avoid electrical charging of the drops, one can notice that the piezoelectric transducer is not directly in contact with the water. Moreover, the net charge of each drop produced by this system has been measured with the help of a faraday pail connected to an electrometer (Keithley model 6514, Sow & Lemaitre, 2016). Regarding the sensitivity of the electrometer (10 fC), no electrical charge was measured on the drop.

Drop size measurements

The generator was calibrated in order to produce drops of a prescribed diameter. Two parameters govern the size of the drops: the water supply pressure and the valve opening time. The different tests performed showed that when the pressure in the water circuit is too high, the drops break-up at the injector outlet. Maintaining pressure below, or at 0.3 bar avoids these effects. These tests were therefore performed at a positive pressure of 0.3 bar. For this water circuit supply pressure, the valve opening time was between 4 and 11 ms. For each opening time, shadowgraph measurements were taken in the aerosol chamber of the BERGAME facility. An example of a shadowgraph image is shown in Figure 3. These measurements were taken after a free-fall acceleration over a height of 8 m.

Atmos. Chem. Phys. Discuss., doi:10.5194/acp-2016-1085, 2017
Manuscript under review for journal Atmos. Chem. Phys.
Published: 5 January 2017

Atmospheric Chemistry and Physics Discussions

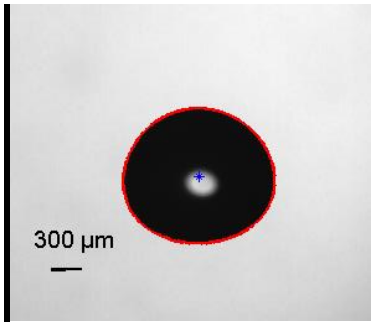

Figure 3. Example of a shadow image

Due to the oscillations of millimetre drops and their lenticular shape, the notion of "diameter equivalent to a sphere of the same volume" has been adopted. With shadowgraphy, yielding only 2-D information, the diameters are equivalent to a disc. Thus, the projected surface area of the drop (S_{goutte}) is measured and the diameter of the disc of equal surface area (D_{eq}) is derived.

$$D_{eq} = \sqrt{\frac{4\,S_{Drop}}{\pi}} \qquad (4)$$

For each injection configuration, the equivalent diameter of the drops is measured for one hundred images. Finally, the mean equivalent diameter and the standard deviation are calculated. Figure 4 shows all the measurement points investigated. For all these operating points, the standard deviation is approximately 20 µm, i.e., approximately 1.5 % of the size of the drop.

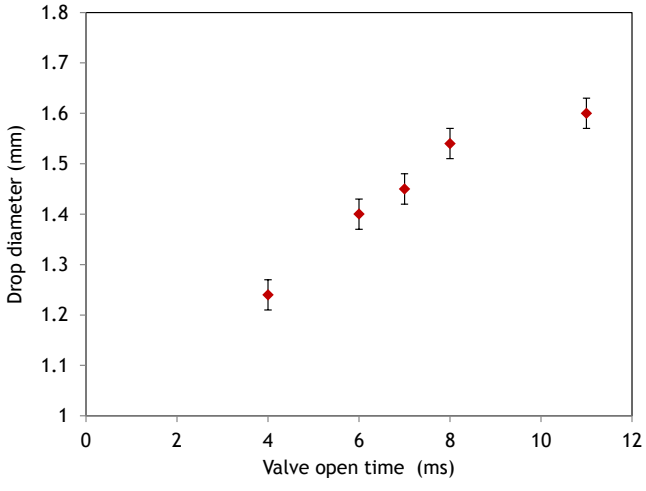

Figure 4. Drop generator setting parameters

Atmos. Chem. Phys. Discuss., doi:10.5194/acp-2016-1085, 2017
Manuscript under review for journal Atmos. Chem. Phys.
Published: 5 January 2017

Atmospheric Chemistry and Physics Discussions

Drop velocity measurements

In order for the drops to be representative of rain, they must cross the BERGAME aerosol chamber at their terminal velocity. For each of the applied settings, the velocity of the drops in the aerosol chamber is measured using the shadowgraphy technique (Figure 3), in taking two consecutive images of the same drop during fall. By measuring the displacement of the centre of the drop between these two images, and knowing the time interval between them, we derive the velocity of the drop. These measurements are shown in Figure 5, where they are compared to the terminal velocity calculated from the Beard (1976) theoretical expression. This theoretical expression relates the size of the drops to their terminal velocity. It is often taken as the reference in the literature as it is verified both in wind tunnel tests and in the environment.

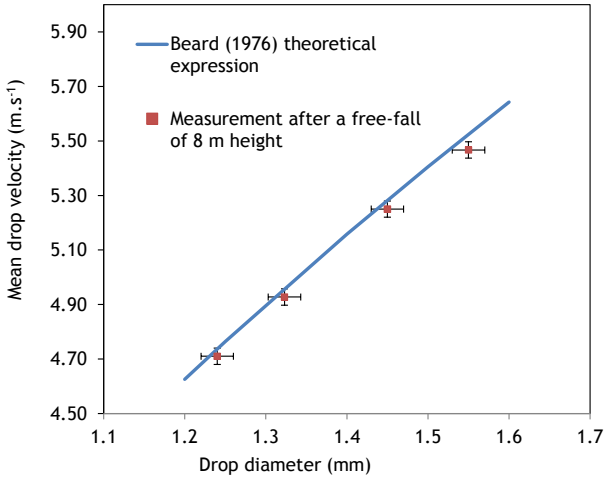

Figure 5. Comparison of velocities measured in BERGAME with the Beard (1976) model

We note in this figure that the 8 m distance is sufficient to accelerate the drops to their terminal velocity. Furthermore, to ensure the representativeness of our drops with respect to the hydrometeors found in the literature, we compare in Figure 6 the axis ratios of the drops in the BERGAME chamber with the model of Beard and Chuang (1987). This figure illustrates that the drops crossing the aerosol chamber are perfectly representative of the hydrometeors found in the atmosphere.

In this study, we focus on the collection efficiency of drops with a diameter of 1.25 mm. We have selected this size, because it is the only one produced by our systems for which comparisons with Beard (1974) simulations can be performed. This model is particularly interesting as we have previously shown, for 2 mm diameter drops (Quérel *et al.* 2014b), that it is the only one able to predict the sharp rise in the collection efficiency observed experimentally for sub-microscopic particles, which is due to the eddies that develop within the wake of the drop. These vortices will capture the particles and draw them back onto the rear of the drop.

Atmos. Chem. Phys. Discuss., doi:10.5194/acp-2016-1085, 2017
Manuscript under review for journal Atmos. Chem. Phys.
Published: 5 January 2017

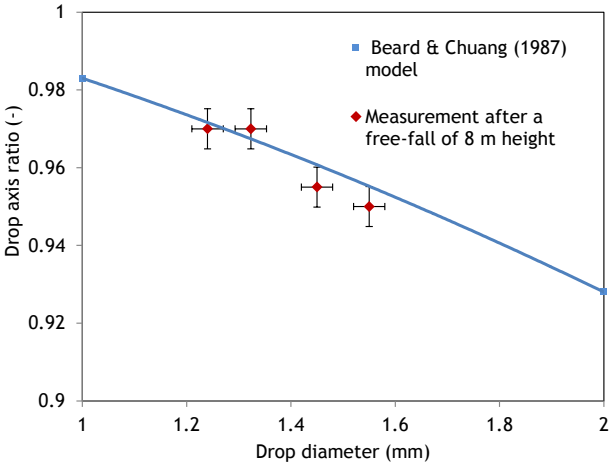

Figure 6. Comparison of axis ratios measured in BERGAME with the model of Beard and Chuang (1987)

2.2 Description of the new BERGAME aerosol chamber

A new aerosol chamber (Figure 7) has been designed to increase the concentration of particles within the volume swept by the drops during their fall. Its geometry is strongly influenced by that developed by Hampl *et al.* (1971). It consists of a 1,300 mm high stainless steel cylinder with an internal diameter of 100 mm.

Various taps are provided for injecting the aerosols, taking samples and characterising the thermodynamic conditions of the gas. These various sampling points serve to measure in particular:

- the aerosol particle size distribution,
- their mass concentration,
- the temperature and relative humidity.

In Figure 7, each valve is labelled with a Greek letter to structure the explanations in the text. The chamber is fitted with two gate valves, one at the top (κ) and the other at the bottom (φ). These two valves isolate the chamber while it is being filled with particles. The particle size distribution of the aerosols is measured by means of an Aerodynamic Particle Sizer (APS, χ) and an Electrical Low Pressure Impactor (ELPI, δ). The injected particles are pure fluorescein particles so that they may be easily measured by fluorescence spectrometry. The mass concentration of the particles in suspension inside the chamber is determined by venting the entire contents of the chamber onto a High Efficiency Particulate Arresting (HEPA) filter (α), and measuring the mass of particles on the filter using fluorescence spectrometry. Finally, the relative humidity and the temperature are given respectively by a capacitive hygrometer and a thermocouple (ω).

Atmos. Chem. Phys. Discuss., doi:10.5194/acp-2016-1085, 2017
Manuscript under review for journal Atmos. Chem. Phys.
Published: 5 January 2017

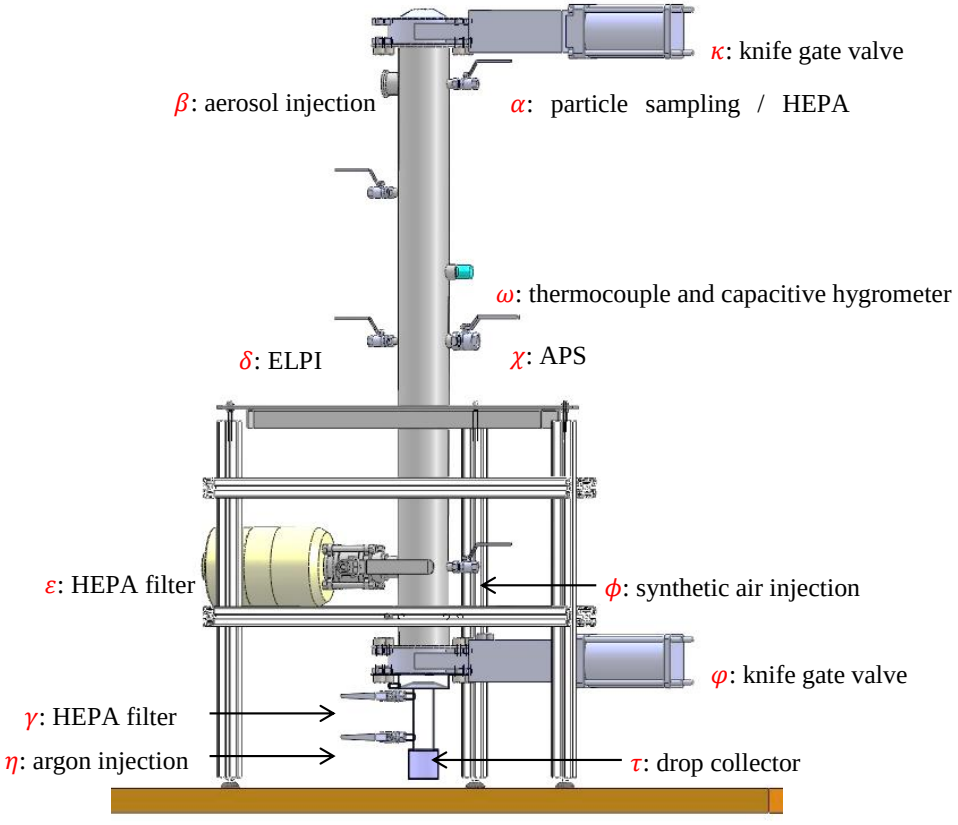

Figure 7. Schematic design of the new BERGAME aerosol chamber

After having accelerated in free fall over 8 m, the drops are representative of rain in terms of size, velocity and axis ratio (section 1.1). They enter the aerosol chamber, via a circular opening with a four centimetres diameter. After crossing the aerosol chamber, the drops are collected in a removable container (τ). One of the principal difficulties of these experiments relates to the sedimentation of the cloud of particles that settles directly inside the drop collector. In order to minimise this sedimentation, a layer of argon (which is denser than the cloud of particles) is formed in the bottom of the aerosol chamber, located below the second gate valve in Figure 7. A large number of experiments were performed. These experiments show that, regardless of the concentration and the size of the particles in the aerosol chamber, until 4 minutes after opening the gate valves, the drop collector is free from any particulate contamination. Beyond four minutes, traces of fluorescein are detected on the drop collector.

Atmos. Chem. Phys. Discuss., doi:10.5194/acp-2016-1085, 2017
Manuscript under review for journal Atmos. Chem. Phys.
Published: 5 January 2017

Atmospheric Chemistry and Physics Discussions

2.3 Aerosol particle generation and characterisation

The aerosol particles are produced with two ultrasound generators. The key part of these generators is a piezoelectric ceramic immersed in a solution. When subjected to an appropriate electric current, this ceramic vibrates at a frequency of 500 or 2 400 kHz depending on the generator used.

These oscillations transform the surface of the liquid into a mist of microscopic droplets with a narrow size distribution. These drops are transported to the upper part of the generator, by a flow of dry filtered air at a flow rate of 20 L.min^{-1}. More dry air is added in the upper part of the generator at a flow rate of 30 L.min^{-1} to dry the particles.

These drying and dispersal flow rates have been selected to obtain the following characteristics:

- the aerosol particle size distributions are narrowly spread (geometric standard deviation less than or equal to 1.5),
- the particle concentration inside the aerosol chamber is high (~ 2 x 10^5 particles.cm^{-3}),
- the relative humidity measured in the aerosol chamber is approximately 77 ± 1 %. This humidity corresponds to relative humidities observed during rainfall events (Depuydt *et al.*, 2012).

Changing the concentration of the solute dissolved in the water varies the size of the particles created, simply change the concentration of solute dissolved in the water. The solute chosen is sodium fluorescein ($C_{10}H_{10}Na_2O_5$). This molecule has been selected for its very large fluorescence properties. It can be easily detected by fluorescence spectroscopy down to a concentration of 5x10^{-11} g.mL^{-1}. Figure 8 shows the particle size distributions of fluorescein measured in the BERGAME aerosol chamber.

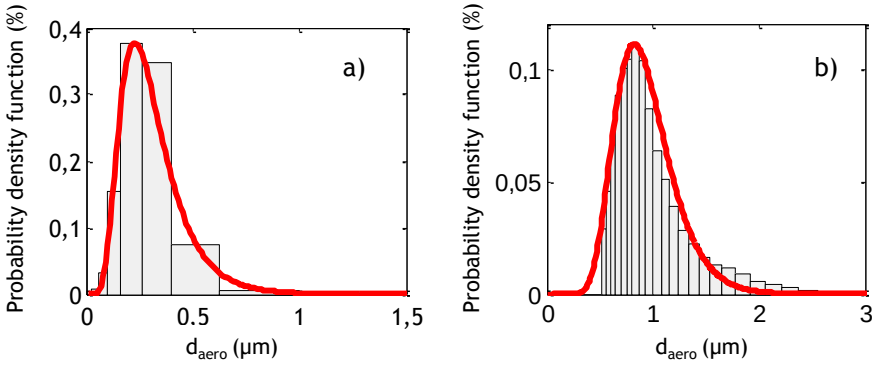

Figure 8. The size distribution of the particles produced by the ultrasound aerosol generator vibrating at 2400 kHz: a) for a fluorescein concentration of 0.11 g.L^{-1} b) for a fluorescein concentration of 10 g.L^{-1}

The distribution on the left is measured using an Electrical Low Pressure Impactor (ELPI, δ) and that on the right using an Aerodynamic Particle Sizer (APS, χ). Both of these distributions show a good fit to log-normal distribution (red curves on the graphs). For a fluorescein concentration of 0.11 g.L^{-1} (respectively 10 g.L^{-1}) in the solution, the median diameter of the fitted distribution is 220 µm (respectively 820 µm) and the geometric standard deviation is 1.5 (respectively 1.34). The generator is placed inside a negative pressure enclosure to prevent any possible fluorescein particle contamination of the laboratory.

Atmos. Chem. Phys. Discuss., doi:10.5194/acp-2016-1085, 2017
Manuscript under review for journal Atmos. Chem. Phys.
Published: 5 January 2017

Atmospheric Chemistry and Physics Discussions

In order to neutralise the charge of the aerosol particles prior to injecting them into the BERGAME aerosol chamber (β), the particles go through a low energy X-ray neutraliser (< 9.5 keV, TSI 3088), at a flow rate of 1.5 L.min^{-1}. At this flow rate, the residence time of the particles in the neutraliser is sufficient to neutralise them.

As we have seen in the previous section, our aerosol generator produces aerosols at a flow rate of 50 L.min^{-1} (20 L.min^{-1} of dispersion air and 30 L.min^{-1} of drying air). We therefore use a flow divider to ensure that the particles pass through the neutraliser at 1.5 L.min^{-1}. This divider comprises an 8 litre buffer volume, provided with one inlet and two outlets. A flow rate of 48.5 L.min^{-1} is drawn-off from one of these outlets means of an air suction pump. This flow is filtered and vented. The remaining flow passes through the neutraliser. After neutralisation, the particles are injected into the aerosol chamber.

2.4 Test procedure

The aerosol chamber is flushed at the start of each experiment with synthetic air, to ensure that initial conditions are free of any fluorescein particle contamination. After flushing, the previously neutralised aerosols particles of the desired diameter are injected at a flow rate of 1.5 L.min^{-1} via valve β (section 1.3: Aerosol particle generation and characterisation).

The two knife gate valves (φ and κ) are closed during this filling phase in order to isolate the enclosure. In addition, valve ε is opened to vent excess pressure towards a HEPA filter. The injection process lasts 20 minutes, during which we form a layer of argon within the zone located below knife gate valve φ. This injection is carried out in two stages. Firstly, we inject the argon during 10 minutes via valve η, with the drop collector is unscrewed and valve γ is closed. During the second phase, the drop collector is refitted and valve γ is opened. At the end of this phase, the aerosol chamber is filled with neutralised particles of the desired diameter, at a concentration of approximately 2x10^5 particles per cubic centimetre.

This enclosure filling phase is followed by a relaxation period lasting no less than 15 minutes. During this period, all the valves of the aerosol chamber are closed with the exception of valve ε, which remains open in order to perfectly balance the pressures. This period is used to align the train of drops produced by the generator with the centreline of the aerosol chamber. Once the drop generator is adjusted, valve ε is closed and both knife gate valves (φ and κ) are opened to enable the drops to cross the aerosol chamber. A volume of 1 cm^3 is necessary for performing a measurement by fluorescence spectrometry, i.e., approximately 1000 drops of 1.25 mm diameter. As a result of the frequency at which the drops cross the enclosure, 10 minutes are needed to collect this volume. As mentioned above, the drop collector remains free of any particulate contamination if the valves remain open for less than 4 minutes. The 10 minutes needed to collect the 1000 drops are therefore divided into 3 periods of 200 seconds each. At the end of these 200 seconds phases, the gate valves are closed again and the buffer volume between gate valve φ and the drop collector is flushed with argon (Figure 9). During flushing, the argon is injected through valve η and removed through valve γ, which ensures an upward flow within this buffer volume and minimises the risk of contamination of the drop collector.

Atmos. Chem. Phys. Discuss., doi:10.5194/acp-2016-1085, 2017
Manuscript under review for journal Atmos. Chem. Phys.
Published: 5 January 2017

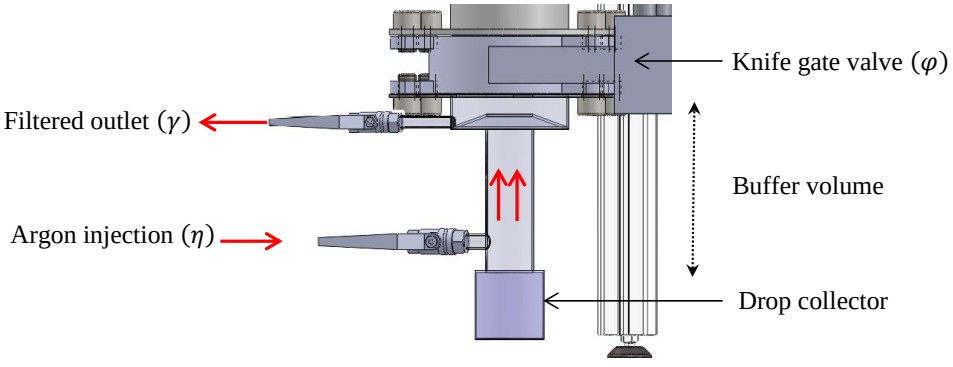

Figure 9. Buffer volume flushing procedure

Once 1 cm^3 of drops have been collected, both knife gate valves are closed, and the buffer volume is flushed, to avoid any contamination of the collected water when removing the drop collector.

In order to determine the collection efficiency, we need to know the mass concentration of fluorescein within the volume swept by the drops (eq. 3). In order to determine this concentration, the aerosol chamber of the BERGAME experiment is flushed with synthetic air at the end of each experiment. This is done by injecting the synthetic air through valve ϕ, at a flow rate of 5 $L.min^{-1}$ during 10 minutes, and collecting the particles on a HEPA filter.

This filter is then placed in 100 mL of ammonia water (V_{sol}) for 24 hours in order to dissolve all the fluorescein particles it contains. Finally, the mass concentration of fluorescein in this water ($[fluo]_{filter}$) is measured by fluorescence spectrometry.

The mass concentration of fluorescein particles in the aerosol chamber ($[fluo]_{chamber}$) is then determined from the following equation:

$$[fluo]_{chamber} = \frac{[fluo]_{filter} \cdot V_{sol}}{V_{chamber}} \quad (5)$$

In this equation, the term $V_{chamber}$ is the volume of the aerosol chamber, i.e. 10.2 L.

As the mass concentration of particles is only quantified once the measurements are completed, we have attempted to quantify its variation over the duration of a measurement (approximately 15 min). For this, we have first verified the stability of production of the aerosol generator, in size and in number. We have then compared the mass concentration in the aerosol chamber just after the relaxation phase and after a complete measurement procedure. At last, measured a reduction in concentration of less than 8 % regardless of the particle diameter. These particles are essentially lost through deposition on the sides of the aerosol chamber.

The collection efficiency is defined as the ratio between the mass of particles (of a given diameter) collected by a drop as it falls, and the total mass of particles (of the same diameter) within the volume it has swept. The mass of fluorescein in the drops during the experiments (M_{drop}) is easy to calculate:

$$M_{gtte} = \frac{\pi D_{drop}^3}{6} [fluo]_{drop} \quad (6)$$

Atmos. Chem. Phys. Discuss., doi:10.5194/acp-2016-1085, 2017
Manuscript under review for journal Atmos. Chem. Phys.
Published: 5 January 2017

Atmospheric Chemistry and Physics Discussions

As is the mass of particles within the volume swept by the drops(M_2):

$$M_2 = \frac{\pi D_{drop}^2 H}{4}[fluo]_{chamber} \qquad (7)$$

The collection efficiency is derived from the following expression:

$$E\left(d_{aero}, D_{drop}, RH\right) = \frac{2\, D_{drop}.[fluo]_{drop}}{3H.[fluo]_{chamber}} \qquad (8)$$

In order to precisely determine the size distribution of the particles for which the collection efficiency has been measured, we repeat the injection of particles into the BERGAME aerosol chamber following each efficiency measurement under exactly the same operating conditions (same generator, same ceramic excitation frequencies, dame injection times, same dispersal and drying flow rates and same fluorescein concentration). The size distribution of the aerosol particles produced by the generator is then measured in the aerosol chamber. For particles with a median diameter less than 0.8 µm, the size distribution is measured using an Electrical Low Pressure Impactor (ELPI). For the others, we favour the use of an Aerodynamic Particle Sizer (APS) because of the larger number of classes.

3 Results and Discussion

All the measurements taken are summarised in Table 1, below. The expanded relative measurement uncertainty of the collection efficiency ($U_{R,E(d_{aero},D_{Drop},RH)}$) is presented in the last column of this table. Its calculation is detailed in Appendix 1 (Lira, 2002).

Table 1. Summary of measurements performed

d_{aero} (µm)	D_{Drop} (mm)	RH (%)	$[fluo]_{drop}$ (g.cm^{-3})	$[fluo]_{chamber}$ (g.cm^{-3})	E (-)	$U_{R,E(d_{aero},D_{Drop},RH)}$ (-)
0.25	1.25	77	8.22 x 10^{-8}	6.22 x 10^{-9}	8.8 x 10^{-3}	4.5 x 10^{-4}
0.25			1.15 x 10^{-7}	7.91 x 10^{-9}	9.7 x 10^{-3}	5.5 x 10^{-4}
0.5			3.39 x 10^{-8}	4.22 x 10^{-9}	5.4 x 10^{-3}	3.4 x 10^{-4}
0.6			4.51 x 10^{-8}	1.38 x 10^{-8}	2.2 x 10^{-3}	1.4 x 10^{-4}
0.71			2.15 x 10^{-8}	9.62 x 10^{-9}	1.5 x 10^{-3}	9.5 x 10^{-5}
1			2.52 x 10^{-7}	1.17 x 10^{-9}	2.9 x 10^{-3}	1.8 x 10^{-4}
1.47			5.48 x 10^{-8}	6.39 x 10^{-9}	5.7 x 10^{-3}	3.6 x 10^{-4}
2.54			6.51 x 10^{-7}	5.51 x 10^{-9}	7.9 x 10^{-2}	5 x 10^{-3}

Atmos. Chem. Phys. Discuss., doi:10.5194/acp-2016-1085, 2017
Manuscript under review for journal Atmos. Chem. Phys.
Published: 5 January 2017

Atmospheric Chemistry and Physics Discussions

In this table, the aerosol diameter (d_{aero}) is the median aerodynamic diameter of each particle size distribution measured using the APS or the ELPI. This aerodynamic diameter is converted into a physical diameter (d_{ap}) by means of the following expression:

$$d_{ap} = d_{aero}\sqrt{\frac{C_{c,d_{aero}}}{C_{c,d_{ap}}}\left(\frac{\rho_0}{\rho_p}\right)} \quad (9)$$

In this equation is the C_c is the Cunningham slip correction factor. The density of the particle (ρ_p) is calculated from the growth factor (*GF*) of the fluorescein aerosol particle.

$$\rho_p = \frac{\rho_{C_{10}H_{10}Na_2O_5} + \rho_0(GF^3 - 1)}{FG^3} \quad (10)$$

This factor has previously been measured using a Hygroscopicity Tandem Differential Mobility Analyser (HTDMA, Quérel *et al.*, 2014b). For our experiments, performed at a relative humidity of 77 ± 5%, we deduce a growth factor (GF) of 1.25 ± 0.05. Stober and Flachsbart (1973) have measured a density of 1.58 g.cm^{-3} for a dry fluorescein aerosol particle. Using equation 10, we therefore calculate the density of our aerosol in the aerosol chamber to be 1.3 ± 0.05 g.cm^{-3}.

The aerodynamic diameters measured in the aerosol chamber by the APS and the ELPI can then be expressed as physical diameters (d_{ap}):

$$d_{ap} = 0.88 \times d_{aero} \quad (11)$$

All our measurements are summarised in Figure 10. In this figure, the x axis is the median diameter of the particles' physical diameter distribution. Our measurements are then compared against the models of Slinn (1977) and Beard (1974). It should be remembered that the Slinn model is currently the model of reference in the environment (Laakso *et al.*, 2003; Chate, 2005). For aerosol particles with diameter in the accumulation mode, the measured collection efficiencies vary considerably with the particle size. On a logarithmic scale, the efficiency curve obtained has a "V" shape with a minimum around 0.65 µm. The increase in collection efficiency for particles larger than 0.65 µm is attributed to the mechanism of impaction on the front face of the drop. Within this size range, the increase in the diameter of the particle increases its inertia. The particle can then no longer follow the streamlines and impacts the drop.

The reasons for the increase in collection efficiency for particles smaller than 0.65 µm in diameter are not as easy to figure out. The Slinn model does not predict this increase and underestimates the collection efficiency for a 0.22 µm particle by two orders of magnitude. This is linked to the assumptions of Stokes flow around the drop. Yet, at Reynolds numbers larger than 20 (a 280 µm drop at its terminal velocity), recirculation eddies develop in the wake of the drop. Beard (1974) has shown the major influence of these wake vortices on the collection of submicron-sized particles. In fact, he showed that the smallest aerosol particles are trapped in these eddies in the wake of the drop then collected on its rear face.

This model is not referred to in the literature as it has never been validated by experiment until now. Yet we observe that, for particles below this minimum efficiency, our measurements are in almost perfect agreement with the model and seem to validate it.

Atmos. Chem. Phys. Discuss., doi:10.5194/acp-2016-1085, 2017
Manuscript under review for journal Atmos. Chem. Phys.
Published: 5 January 2017

Atmospheric Chemistry and Physics Discussions

For particles with a diameter greater than 1 µm, we observe that the Beard or Slinn models yielded almost the same values. This result is expected since their only difference stands in the Stokes flow around the drop for Slinn model. This assumption prevents the capture of boundary layer separation in the wake of the drop and the resulting recirculating flows even if it makes very little difference to the flow on the leading edge of the drop. Yet particles with a diameter greater than 1 µm are very sensitive to inertial effects and are captured on this front face. Moreover as the Stokes number of these large particles is high, they pass through these recirculations without being trapped.

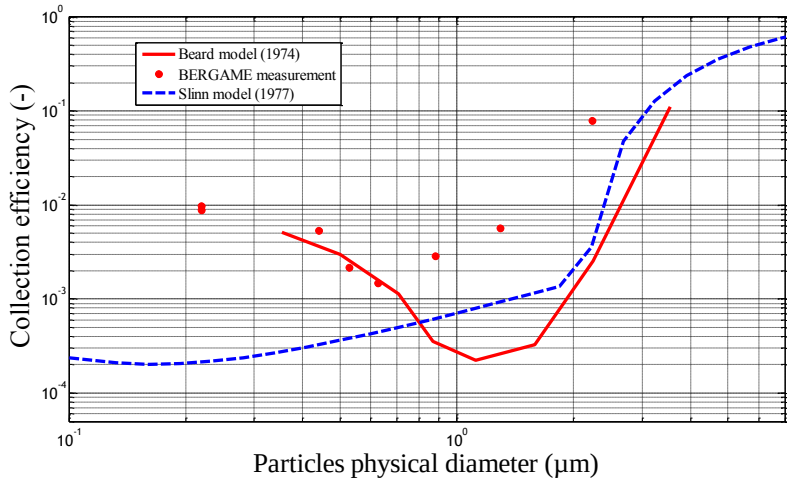

Figure 10. Comparison of our measurements for a drop of 1.25 mm diameter with the models of Beard (1974) and Slinn (1977)

For particles with a diameter greater than 0.65 µm, our measurements show the same trends as these two models but with an average difference of one order of magnitude. This is probably related to the fact that, during our experiments, the aerosol particles in the aerosol chamber are not perfectly mono-disperse. In fact, the particles have log-normal distributions with geometric standard deviations between 1.3 and 1.5 (Figure 8). The collection efficiency varies very sharply with particle size. Thus, in order to compare more rigorously our measurements with the model, we need to calculate, for each measurement, the average theoretical collection efficiency $(\langle E(D_{gtte}, d_{ap})\rangle)$ of Beard (1974) resulting from the entire range of particle sizes in the aerosol chamber (Eq. 12).

$$\langle E(D_{gtte} = 1.25\ mm, d_{ap})\rangle = \frac{\int_{d_{ap=0}}^{\infty} f(d_{ap}).\, d_{ap}^3.\, E(D_{gtte} = 1{,}25\ mm, d_{ap})\mathrm{d}d_{ap}}{\int_{d_{ap=0}}^{\infty} f(d_{ap}).\, d_{ap}^3.\, \mathrm{d}d_{ap}} \quad (12)$$

In this equation, the term $f(d_{ap})$ is the probability density function of the particles in the BERGAME aerosol chamber, and $E(D_{gtte} = 1.25\ mm,\ d_{ap})$ is the collection efficiency calculated by the Beard model (1974) for a

Atmos. Chem. Phys. Discuss., doi:10.5194/acp-2016-1085, 2017
Manuscript under review for journal Atmos. Chem. Phys.
Published: 5 January 2017

Atmospheric Chemistry and Physics Discussions

drop 1.25 mm in diameter. The numerator and denominator of this equation are both weighted by a term d_{ap}^3, which reflects the fact that, experimentally, we measure intensities of fluorescence, and therefore masses of particles. We use the rectangle method to numerically solve this integral. In addition, the functions $E(D_{gtte} = 1.25\ mm,\ d_{ap})$ and $f(d_{ap})$ are both interpolated using Hermite interpolation polynomials (Fritsch et Carlson, 1980) with a step size of 0.1 µm.

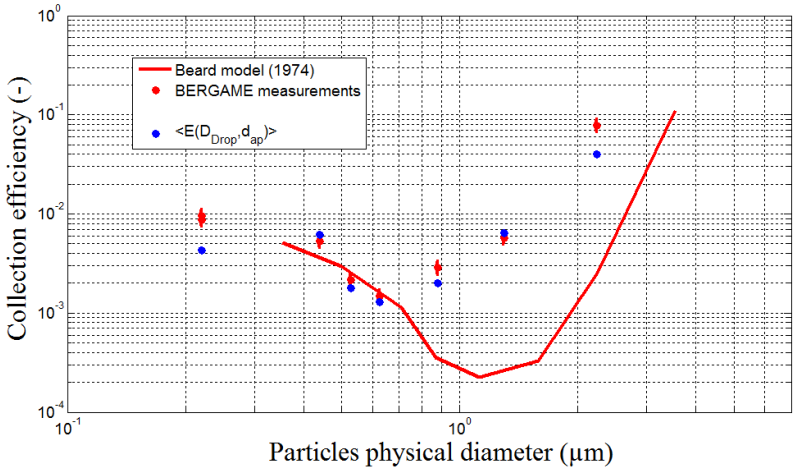

Figure 11. Integration of the Beard (1974) model over the particle size distribution of each of our experiments, for a drop of 1.25 mm diameter

We note a significant improvement of the agreement between our measurements and the Beard (1974) model integrated over the entire particle distribution during our experiments in BERGAME (Figure 11). Larger differences are nevertheless observed for the first ($d_{ap} = 0.22\ \mu m$) and last measurement points ($d_{ap} = 2.54\ \mu m$). These larger differences are attributed to the fact that, for these points, the resolution of equation (12) requires an interpolation of the Beard (1974) model within a particle size range without any calculation point. Based on these comparisons, we can consider that the Beard (1974) model is validated for addressing the collection by raindrops of the aerosol particles of the accumulation mode.

Therefore, in order to estimate accurately the collection by raindrops, it is essential to take account of rear capture which is both theoretically predicted and observed in these measurements. Neglecting rear capture can result in an error of two orders of magnitude in the collection efficiency for a 1.25 mm drop.

In order to compile a semi-empirical expression to quantifying the elementary collection efficiency resulting from rear capture alone ($E_{rear\ capture}$), we display in Figure 12 the collection efficiencies numerically simulated by Beard (1974) as a function of the drops Reynolds number and the Stokes number of the particles. These plots are limited to the range of particle Stokes numbers for which the level of rear capture is high.

Atmos. Chem. Phys. Discuss., doi:10.5194/acp-2016-1085, 2017
Manuscript under review for journal Atmos. Chem. Phys.
Published: 5 January 2017

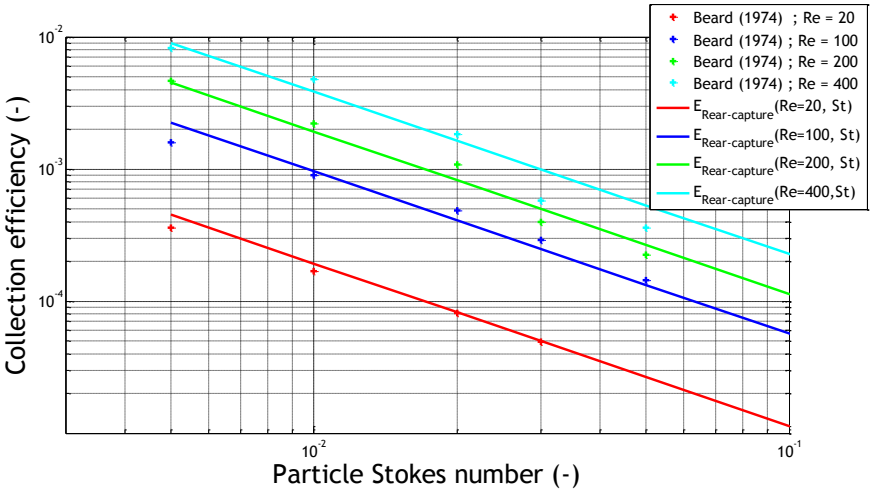

Figure 12. Semi-empirical parametrization of rear capture

This figure suggest that Reynolds number of the drop and Stokes number of the aerosol particles are the two parameters influencing rear capture. The dependency on these two dimensionless numbers is physical as the Reynolds number of the drop (Re_{Drop}) reflects the intensity and the size of the areas of recirculating flow in its wake; and the particle Stokes number (St_{ap}) reflects the susceptibility of the particle pass through the recirculating flow in the wake of the drop without being trapped.

Applying a power law fit to the simulations of Beard (1974) yields equation 13.

$$E_{rear-capture} = \frac{1}{3\times10^{7}} Re_{Drop} \times St_{ap}^{-1.23} \quad (13)$$

This correlation is presented in solid lines in Figure 12 and shows a satisfactory agreement with K.V. Beard simulations in the corresponding range of drop Reynolds number and particle Stokes number.

However, it should be kept in mind that this relationship is only valid for drop Reynolds numbers larger than 20 (a 280 µm drop at its terminal velocity), as below this critical value there is no recirculating flow behind the drop (Le Clair *et al.* 1972).

Conclusion

This study is a follow up of the paper by Quérel *et al.* (2014b) and treats questions raised therein. In particular, Quérel *et al.* (2014b) showed that their efficiency measurements of submicron particles could only be explained by rear capture. This paper confirms the impact of recirculating flows at the rear of the drop on the collection of submicron particles. This was done by directly comparing our measurements against the numerical simulations of Beard (1974). The BERGAME experimental setup was optimised to considerably reduce the measurement uncertainties, as well as to perfectly control the electric charges of both the drops and the aerosol particles.

As in Quérel *et al.* (2014b), we show that the collection efficiency of the accumulation mode aerosol particles by drops representative of rain varies significantly with the size of the particles. On a logarithmic scale, the

Atmos. Chem. Phys. Discuss., doi:10.5194/acp-2016-1085, 2017
Manuscript under review for journal Atmos. Chem. Phys.
Published: 5 January 2017

Atmospheric Chemistry and Physics Discussions

efficiency curve obtained shows a "V" shape with a minimum around 0.65 µm. The increase in collection efficiency for particles larger than 0.65 µm is attributed to the mechanism of impaction on the front face of the drop. Within this size range, the increase in the diameter of the particle increases its inertia, and the particle can no longer follow the streamlines, and thus impacts the drop. As not possible for the measurements of Quérel *et al.* (2014b), we can now directly compare our results with the numerical simulations carried out by Beard (1974). This comparison highlights the robustness of his model for predicting the efficiency of capture of particles by raindrops over the entire accumulation mode. It should be noted that only this model predicts the significant increase in collection efficiency that we measured for submicron particles. This is related to the fact that Beard (1974) first simulated the flow around the drop by solving the complete Navier-Stokes equation (without ignoring the convection terms; Beard and Grover, 1974). He, therefore, captures the separation of the boundary layer at the rear of the drop and the resulting recirculating flows; and then, he simulates the trajectory of the particles in this velocity field. Beard thus shows that the increase in the collection efficiency of submicron particles as observed in experiments is due to the fact that these particles are captured in the recirculating flows to the rear of the drop and drawn back into its rear face.

Furthermore, we have also shown that, for particles larger than one micrometre, the models of K.V. Beard and W.G.N. Slinn are very similar. Finally, we propose a new semi-analytical expression to calculate the elementary efficiency of capture by the rear recirculating flows. It is important that this mechanism should be systematically taken into account to avoid errors of at least two orders of magnitude on the collection efficiency and consequently on the scavenging coefficient.

In the near future, we plan to integrate these new measurements within the DESCAM model (Flossmann, 1986; Flossmann, 1991; Querel et al 2014a) and to compare the scavenging coefficient derived from the theoretical approaches and derived from the experiments conducted in the environment by Volken and Shuman (1993), Laakso *et al*. (2003) and Chate (2005).

Finally, we plan, in a more distant future, to look at other hydrometeors such as snow and hail.

Appendix 1: Evaluation of uncertainties

The collection efficiency is calculated by means of equations (3) and (6) from which we derive the equation below, by substitution:

$$E\left(d_{aero}, D_{Drop}, RH\right) = \frac{2\, D_{Drop}.[fluo]_{Drop}.V_{chamber}}{3H.[fluo]_{filter} \cdot V_{sol}}$$

The expanded relative measurement uncertainty of the collection efficiency ($U_{R,E(d_{aero},D_{Drop},RH)}$) is determined with the help of the law of propagation of variances, considering an expansion factor of two (Lira, 2002) :

$$U_{R,E(d_{aero},D_{Drop},RH)} = 2\sqrt{u^2_{R,\,D_{Drop}} + u^2_{R,[fluo_{Drop}]} + u^2_{R,V_{chamber}} + u^2_{R,H} + u^2_{R,[fluo_{filter}]} + u^2_{R,V_{sol}}}$$

Atmos. Chem. Phys. Discuss., doi:10.5194/acp-2016-1085, 2017
Manuscript under review for journal Atmos. Chem. Phys.
Published: 5 January 2017

Atmospheric Chemistry and Physics Discussions

In the right-hand member of this expression, the terms $u_{R,X}$ correspond to the relative measurement uncertainty of X. Each experimental uncertainty is discussed in a separate sub-section.

Uncertainty in drop size

Shadowgraph measurements of the size of the drops have shown that our drop generation system is very stable and reproducible for the parameters adopted (section 1.1). The standard deviation of the drop size distribution is 20 µm; we use this standard deviation to determine the relative uncertainty in the diameter of the drops.

$$u_{R,\,D_{Drop}} = \frac{\sigma_{D_{Drop}}}{D_{Drop}} = \frac{20 \times 10^{-3}}{1{,}3} \approx 0{,}015$$

Uncertainty in fluorescein concentration measurements

For the range of concentrations within which fluorescence spectrometry is used, the calibration certificate of the spectrometer indicates an expanded relative measurement uncertainty ($U_{R,[fluo_{gtte}]}$) of less than five percent. We then derive the relative measurement uncertainty of the fluorescein concentration in the drops ($u_{R,[fluo_{Drop}]}$):

$$u_{R,[fluo]_{Drop}} = \frac{U_{R,[fluo]_{Drop}}}{2} \approx 0{,}025$$

For the fluorescein concentration measured in the aerosol chamber($[fluo_{chamber}]$), we have the same uncertainty associated with the fluorescence spectrometry measurement. In addition to this measurement uncertainty, there is a second uncertainty associated with the reduction in concentration during the course of the experiment. We have calculated this reduction to be less than eight percent over the duration of the measurement. The total relative uncertainty in the fluorescein concentration inside the aerosol chamber is therefore approximately 8 % (equation below).

$$u_{R,[fluo]_{chamber}} = \sqrt{0{,}025^2 + 0{,}08^2} \approx 0{,}08$$

Uncertainty in height of aerosol chamber

The aerosol chamber measures 1.3 metres plus or minus 1 millimetre. However, over the duration of the measurement, the particles diffuse and move slightly outside the geometric boundaries of the aerosol chamber. We calculate the maximum error in the height of interaction between the drops and the particles (EMT_H) to be approximately two centimetres (one above and one below the chamber). We therefore calculate the relative uncertainty for this height of interaction ($u_{R,H}$) by means of the following equation:

$$u_{R,H} = \frac{EMT_H}{3\,H} \approx 0{,}005$$

Atmos. Chem. Phys. Discuss., doi:10.5194/acp-2016-1085, 2017
Manuscript under review for journal Atmos. Chem. Phys.
Published: 5 January 2017

Atmospheric Chemistry and Physics Discussions

Uncertainty in volume of dilution:

The uncertainty in the volume of dissolution is very low, we estimate its maximum error ($EMT_{V_{sol}}$) to be one millimetre. We derive a relative uncertainty in the dilution ($u_{R,V_{sol}}$):

$$u_{R,V_{sol}} = \frac{EMT_{V_{sol}}}{3\,V_{sol}} \approx 0{,}003$$

Uncertainty in volume of aerosol chamber

The uncertainty in the volume of the aerosol chamber is low, we estimate its maximum error ($EMT_{V_{chambre}}$) to be 20 centilitres. We derive the relative uncertainty in the dilution ($u_{R,V_{chamber}}$):

$$u_{R,V_{chamber}} = \frac{EMT_{V_{chamber}}}{3\,V_{chamber}} = \frac{20 \times 10^{-2}}{3 \times 10} \approx 0{,}007$$

Uncertainty in relative humidity

The relative humidity is not directly involved in the calculation of collection efficiency. However, it is established, for the finest droplets, that the efficiency increases considerably when the relative humidity reduces, due to diffusiophoresis. For example, Grover *et al.* (1977) calculated that the collection efficiency of a 0.5 µm aerosol particle by a 80 µm, can increase by a factor of 10^4 when the relative humidity falls from 100 to 20%.

However, our recent measurements, for the largest hydrometeors forming rain (between 2 and 2.6 mm; Quérel *et al.*, 2014b) showed no dependency of the collection efficiency on relative humidity.

During our experiments, the aerosol generator settings were optimised in such a way that, at the end of the aerosol chamber filling phase, the relative humidity in the chamber was 75 ± 1 %.

For each measurement, during the 10 minutes needed to collect one millilitre of drops (section 2), the relative humidity increased by 5 ± 1 %. This increase is related to an accumulation of water on the slightly inclined bottom of the aerosol chamber.

We consider therefore that the measurement uncertainty for the relative humidity is approximately 5 %.

References

Beard, K. V. (1974). Experimental and numerical collision efficiencies for submicron particles scavenged by small raindrops. *Journal of the Atmospheric Sciences*, *31*(6), 1595-1603.

Beard, K. V. and Grover, S. N. (1974). Numerical collision efficiencies for small raindrops colliding with micron size particles. *Journal of the Atmospheric Sciences*, *31*(2), 543-550.

Beard, K. V. (1976). Terminal velocity and shape of cloud and precipitation drops aloft. *Journal of the Atmospheric Sciences*, *33*(5), 851-864.

Beard, K. V., and Chuang, C. (1987). A new model for the equilibrium shape of raindrops. *Journal of the Atmospheric sciences*, *44*(11), 1509-1524.

Charlson, R. J., Schwartz, S. E., Hales, J. M., Cess, R. D., Hansen, J. E., and Hofmann, D. J. (1992). Climate Forcing by Anthropogenic Aerosols. *Science*, 255 (5043), 423-430.

Chate, D. M. (2005). Study of scavenging of submicron-sized aerosol particles by thunderstorm rain events. *Atmospheric Environment*, *39*(35), 6608-6619.

Depuydt, G. (2013). *Etude expérimentale in situ du potentiel de lessivage de l'aérosol atmosphérique par les précipitations* (Doctoral dissertation, available from Toulouse University).

Depuydt, G., Masson, O., Gomes, L., and Brenguier, J. L. (2012). Micro and macro-physical characterizations of precipitations in continental and Mediterranean environments. In 16th International Conference on Clouds and Precipitation, ICCP-2012, July 30 – August 3, 2012, Leipzig, Germany.

Flossmann, A. I. (1986). A theoretical investigation of the removal of atmospheric trace constituents by means of a dynamic model, Ph.D. thesis, 186 pp., Phys. Dep., Johannes Gutenberg-Univ. Mainz, Mainz, Germany.

Flossmann, A. I. (1991). The scavenging of two different types of marine aerosol particles calculated using a two-dimensional detailed cloud model, *Tellus*, 43B, 301–321.

Fritsch, F. N., and Carlson, R. E. (1980). Monotone piecewise cubic interpolation.*SIAM Journal on Numerical Analysis*, *17*(2), 238-246.

Groëll, J., Quélo, D., and Mathieu, A. (2014). Sensitivity analysis of the modelled deposition of 137 Cs on the Japanese land following the Fukushima accident.International Journal of Environment and Pollution, 55(1-4), 67-75.

Grover, S. N., Pruppacher, H. R., and Hamielec, A. E. (1977). A numerical determination of the efficiency with which spherical aerosol particles collide with spherical water drops due to inertial impaction and phoretic and electrical forces. *Journal of the Atmospheric Sciences*, *34*(10), 1655-*1663.*

Hampl, V. M. D. D. E., Kerker, M., Cooke, D. D., and Matijevic, E. (1971). Scavenging of aerosol particles by a falling water droplet. Journal of the Atmospheric Sciences, 28(7), 1211-1221.

Jaenicke, R. (1988). Aerosol physics and chemistry. *Zahlenwerte und Funktionen aus Naturwissenschaften und Technik*, *4*, 391-457.

Kerker, M., and Hampl, V. (1974). Scavenging of Aerosol Particles by a Failing Water Drop and Calculation of Washout Coefficients. *Journal of the Atmospheric Sciences*, *31*(5), 1368-1376.

Laakso, L., Grönholm, T., Rannik, Ü., Kosmale, M., Fiedler, V., Vehkamäki, H., and Kulmala, M. (2003). Ultrafine particle scavenging coefficients calculated from 6 years field measurements. *Atmospheric Environment*, *37*(25), 3605-3613.

Lai, K. Y., Dayan, N., and Kerker, M. (1978). Scavenging of aerosol particles by a falling water drop. *Journal of the Atmospheric Sciences*, *35*(4), 674-682.

Le Clair, B. P., Hamielec, A. E., Pruppacher, H. R., and Hall, W. D. (1972). A theoretical and experimental study of the internal circulation in water drops falling at terminal velocity in air. *Journal of the Atmospheric Sciences*, 29(4), 728-740.

Lira, I. (2002). Evaluating the measurement uncertainty: fundamentals and practical guidance. *Measurement Science and Technology*, 13(9), 1502.

Ménard, T., Tanguy, S., and Berlemont, A. (2007). Coupling level set/VOF/ghost fluid methods: Validation and application to 3D simulation of the primary break-up of a liquid jet. International Journal of Multiphase Flow, 33(5), 510-524.

Mircea, M., and Stefan, S. (1998). A theoretical study of the microphysical parameterization of the scavenging coefficient as a function of precipitation type and rate. *Atmospheric Environment*, *32*(17), 2931-2938.

Mircea, M., Stefan, S., and Fuzzi, S. (2000). Precipitation scavenging coefficient: influence of measured aerosol and raindrop size distributions. *Atmospheric Environment*, *34*(29), 5169-5174.

Pranesha, T. S., and Kamra, A. K. (1996). Scavenging of aerosol particles by large water drops: 1. Neutral case. *Journal of Geophysical Research: Atmospheres (1984–2012)*, *101*(D18), 23373-23380.

Pruppacher, H. R., Klett, J. D., and Wang, P. K. (1998). Microphysics of clouds and precipitation. Kluwer academic publishers, Dordrecht, Boston, London, 852.

Quérel, A., Monier, M., Flossmann, A. I., Lemaitre, P., and Porcheron, E. (2014a). The importance of new collection efficiency values including the effect of rear capture for the below-cloud scavenging of aerosol particles. *Atmospheric Research*, *142*, 57-66.

Quérel, A., Lemaitre, P., Monier, M., Porcheron, E., Flossmann, A. I., and Hervo, M. (2014b). An experiment to measure raindrop collection efficiencies: influence of rear capture. *Atmospheric Measurement Techniques*, *7*(5), 1321-1330.

Quérel, A., Roustan, Y., Quélo, D., and Benoit, J. P. (2015). Hints to discriminate the choice of wet deposition models applied to an accidental radioactive release. *International Journal of Environment and Pollution*, 58(4), 268-279.

Slinn, W. G. N. (1977). Some approximations for the wet and dry removal of particles and gases from the atmosphere. *Water, Air, and Soil Pollution*, *7*(4), 513-543.

Sow, M., and Lemaitre, P. (2016). Influence of electric charges on the washout efficiency of atmospheric aerosols by raindrops. *Annals of Nuclear Energy*, 93, 107-113.

Stöber, W., and Flachsbart, H. (1973). An evaluation of nebulized ammonium fluorescein as a laboratory aerosol. *Atmospheric Environment (1967)*, *7*(7), 737-748.

Szakáll, M., Mitra, S. K., Diehl, K., and Borrmann, S. (2010). Shapes and oscillations of falling raindrops—A review. *Atmospheric research*, *97*(4), 416-425.

Twomey, S. (1974). Pollution and the planetary albedo. *Atmospheric Environment (1967)*, *8*(12), 1251-1256.

Vohl, O., Mitra, S. K., Wurzler, S. C., and Pruppacher, H. R. (1999). A wind tunnel study of the effects of turbulence on the growth of cloud drops by collision and coalescence. *Journal of the Atmospheric Sciences*, *56*(24), 4088-4099.

Volken, M., and Schumann, T. (1993). A critical review of below-cloud aerosol scavenging results on Mt. Rigi. *Water, Air, and Soil Pollution*, *68*(1-2), 15-28.

Atmos. Chem. Phys. Discuss., doi:10.5194/acp-2016-1085, 2017
Manuscript under review for journal Atmos. Chem. Phys.
Published: 5 January 2017

Atmospheric Chemistry and Physics Discussions

Wang, P. K., and Pruppacher, H. R. (1977). An experimental determination of the efficiency with which aerosol particles are collected by water drops in subsaturated air. *Journal of the Atmospheric Sciences*, *34*(10), 1664-1669.

Wang, R., Tao, S., Shen, H., Huang, Y., Chen, H., Balkanski, Y., Boucher, O., Ciais, P., Shen, G. F., Li, W., Zhang, Y. Y., Chen, Y. C., Lin, N., Su, S., Li, B. G., Liu, J. F., and Liu, W. X (2014). Trend in global black carbon emissions from 1960 to 2007. *Environmental science & technology*, 48(12), 6780-6787.

Whitby, K. T. (1973). On the multimodal nature of atmospheric aerosol size distribution. In VIII International Conference on Nucleation, Leningrad, U.S.S.R., September 24-29, 1973.